View metadata, citation and similar papers at core.ac.uk
brought to you by CORE
provided by Elsevier - Publisher Connector

profiles, the MC code used was PENELOPE extended to protons (PENH). The transfer function is obtained from interpolation of a table of analytical fits to previously MC simulated responses of the camera. Optical and spectral properties of the incident proton beam are also taken into account in both MC and analytical models. Neutrons contribute to the total signal as a flat background with notable uncertainties and with no impact on the range shift estimation and are therefore not simulated.The analytical model was benchmarked against MC simulations and experiments for various configurations of a cylindrical phantom with inserts of different tissue-equivalent materials. It was also benchmarked against MC in patients. We present here the results for a critical configuration as shown in the figure (part (b)). The proton incident energy was set to 110 MeV. Protons are expected to stop at the interface between muscle (G452) and lung (LN 300) equivalent tissues.

Results: For the results shown in the figure (part (c)), excellent agreement is observed between the analytical model and MC: 99.7% of the points for PG emission passing a gamma 3%/1 mm criteria and an agreement within 0.6 mm for the estimation of range shifts. Agreement between the analytical model and measurements (MS) is within 0.4 mm for range shifts. The measured signal was corrected for the contribution of the neutrons by matching the average of measured values to the average of MC values. Typical computing time for the analytical model is between 50 to 150 ms for a single spot.

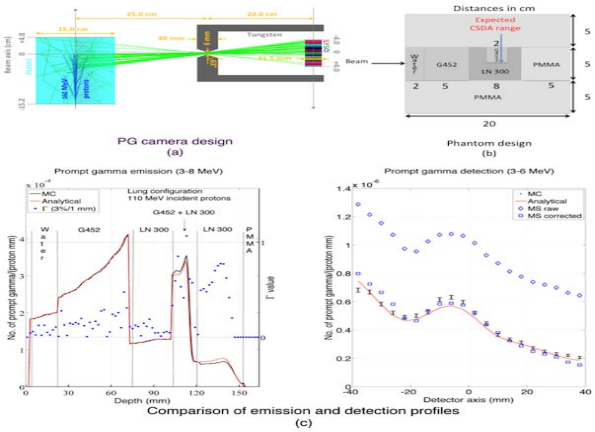

Conclusions: A fast and accurate analytical model has been validated in phantom and CT geometries for an existing prompt gamma camera prototype. The analytical model can now be used for future implementation of the system in clinical practice.

OC-0558

AAPM Task Group 158: measurement approaches for doses outside the treatment volume from external-beam radiation

R.M. Howell[1], B. Bednarz[2], S.F. Kry[1]
[1]*University of Texas MD Anderson Cancer Center, Radiation Physics, Houston, USA*
[2]*University of Wisconsin, Medical Physics, Madison, USA*

Purpose/Objective: Measuring, calculating, and reducing non-target doses present unique challenges with which many medical physicists may have limited experience with. The American Association of Physicists in Medicine Task Group (TG) 158, measurement and calculation of doses outside the treatment volume from external-beam radiation therapy (EBRT), was created to provide guidance for physicists in assessing and managing non-target doses. **The primary objective of this presentation** is to discuss uses of dosimeters and phantoms for measuring non-target doses from photon, electron, and light-ion EBRT.

Materials and Methods: The TG-158 reviewed approximately 300 publications in the literature, twenty percent of which focused on measurement techniques, detectors, and phantoms for assessment of non-target doses. This presentation will highlight key components of Chapter 4 of TG-158 report, measurement approaches.

Results: For measurements of non-target dose in photon and electron therapy, the following detectors will be discussed: thermo luminescent and optically luminescent dosimeters, diodes, metal oxide-silicon semiconductor field effect transistor dosimeters, and ion chambers. The use of each dosimeter will be presented in the context of (1) dose at the surface, (2) energy spectrum, (3) dosimeter dynamic range, and (4) presence of other particles.

This presentation will also summarize various detectors that can be used to measure secondary neutrons. Neutron detectors are highly energy dependent and thus, knowledge of the energy spectrum being measured is essential. The secondary neutrons from electron, photon, and light-ion therapy have a wide energy range, i.e., from thermal up to about 10 MV for photon/electron therapy and thermal up to 250 MeV for light ion therapy. Moreover, many neutron detectors cannot be used in or near the primary field because of issues such as pulse-pile-up and interactions of particles within the detector, among others. Thus, each neutron detector will be presented in the context of its energy sensitivity and its suitability for measurements in-or near the primary field.

Finally, the presentation will highlight various issues related to phantom selection, including assumptions about organ position within anthropomorphic phantoms, adult verses pediatric phantoms, and effect of phantoms on neutron energy spectra.

Conclusions: This presentation will highlight the unique challenges of measuring non-target doses and will provide guidance on how to select the most appropriate detector and phantoms for these measurements for photon, electron, and light-ion therapy.

Proffered Papers: RTT 5: Advanced imaging and volume definition

OC-0559

Reliability and accuracy assessment of RTOG-endorsed guidelines for brachial plexus contouring

T. Vercauteren[1], J. Van De Velde[2], W. De Gersem[1], J. Wouters[2], K. Vandecasteele[1], P. Vuye[1], F. Vanpachtenbeke[1], K. D'Herde[2], I. Kerckaert[2], A. Van Greveling[1], W. De Neve[1], T. Van Hoof[2]
[1]*University Ghent, Radiotherapy, Ghent, Belgium*
[2]*University Ghent, Anatomy, Ghent, Belgium*

Purpose/Objective: Validation of the Radiation Therapy Oncology Group (RTOG)-endorsed guidelines (Table 1) for brachial plexus (BP) contouring by determining the intra- and interobserver agreement. Anatomically validated computed tomography (CT) and magnetic resonance imaging (MRI) datasets were used as a gold standard to determine the accuracy of the delineation process. Validation of the BP was performed by dissection of all cadavers.

Materials and Methods: The right BP was delineated on 3 CT cadaver datasets by 5 observers. Inter- and intraobserver variation was computed using the Computerized Environment for Radiation Research (CERR) package. Each observer

delineated the BP 3 times, every time with an interval of 2 weeks. A detailed statistical analysis was performed on 4 subregions of the BP. The first region extends from the exit of the BP through the intervertebral foramina until the entrance of the scalene opening. The second region ends at the entrance between the subclavius and serratus anterior muscles. The third region was defined between the subclavius and serratus anterior muscles. The fourth region defines the BP bordered between the minor pectoral, subscapular and serratus anterior muscles. The delineation accuracy was determined by measuring the BP inclusion of the delineations on rigidly fused CT-MRI datasets.
Results: A low inter- and intraobserver reliability was observed. The mean inter- and intraobserver kappa was respectively 0.29 and 0.45. The minimum and maximum Jaccard index in the intraobserver group was 0.004 and 0.636 while in the interobserver group 0 and 0.124 was obtained. The total agreement volume in both intra- and interobserver groups was much lower than the union volume. The overall accuracy was poor, with an average inclusion of 38% (Figure 1) . The accuracy of the delineations reduced from the medial to the lateral BP regions.
Conclusions: Poor inter- and intraobserver reliability of the RTOG-endorsed BP contouring guidelines was observed. Accuracy analysis showed an average BP inclusion of 38%. BP inclusion reduced from the medial to the lateral BP regions. Insufficient accuracy and reliability of the RTOG-endorsed BP guidelines was observed.

1	Identify and contour C5, T1, and T2
2	Identify and contour the subclavian and axillary neurovascular bundle
3	Identify and contour anterior and middle scalene muscles from C5 to insertion onto the first rib
4	To contour the brachial plexus OAR use a 5-mm diameter paint tool
5	Start at the neural foramina from C5 to T1; this should extend from the lateral aspect of the spinal canal to the small space between the anterior and middle scalene muscles
6	For CT slices, where no neural foramen is present, contour only the space between the anterior and middle scalene muscles
7	Continue to contour the space between the anterior and middle scalene muscles; eventually the middle scalene will end in the region of the subclavian neurovascular bundle
8	Contour the brachial plexus as the posterior aspect of the neurovascular bundle inferiorly and laterally to one to two CT slices below the sternoclavicular joint and one to two ct slices superior to the level of the top of the aortic arch and the inferior aspect of the glenohomeral joint. The contour should have an approximate transverse length of 3 to 4 cm at this level
9	The first and second ribs serve as the medial and approximate lateral limit of the OAR contour. The contour should not pass inferiorly to the level of the second rib

Table 1 RTOG-endorsed brachial plexus contouring guidelines

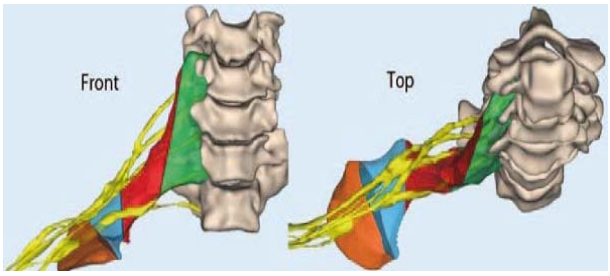

Figure 1 Delineation of the brachial plexus (BP) by one observer on a cadaver dataset. In this example the delineation shows a 38.43% BP (yellow) inclusion. The defined subregions: region 1: green, region 2: red, region 3: blue, region 4: orange.

OC-0560

FIESTA MRI to investigate CSF around lower cranial nerve roots; implications for radiotherapy planning

D. Noble[1], D. Scoffings[2], S.J. Jefferies[1], M.V. Williams[1]
[1]*Addenbrooke's Hospital Oncology Centre, Oncology, Cambridge, United Kingdom*
[2]*Addenbrooke's Hospital Radiology Centre, Neuro-radiology, Cambridge, United Kingdom*

Purpose/Objective: Radiotherapy is a critical treatment for both medulloblastoma and ependymoma. The literature does not assess whether or not to include the roots of posterior fossa cranial nerves (CN's - VII-XII) in the target volume. There is also little data describing the anatomy of cerebrospinal fluid (CSF) as it follows the roots of these CN's, specifically how far it flows into their respective skull base formaniae. The role of MRI, in particular steady-state free precession sequences such as FIESTA, in imaging the cisternal segments of CN's, is well described. This study aims to determine whether a database of FIESTA images can be used to answer this anatomical question and whether this data can be used to guide radiotherapy planning.
Materials and Methods: A database of 97 FIESTA sequences of the posterior fossa was reviewed. Examinations were excluded for these reasons; sagittal reconstructions only, abnormal head shape/anatomy, no FIESTA sequences, limited number of slices pulled from archive, structure not clearly visualized. Measurements were made on the following number of scans for each foramen respectively; 86 left internal acoustic meatus (IAM), 84 right IAM, 83 left jugular foramen (JF), 85 right JF, 42 left hypoglossal canal (HC), 45 right HC. A protocol was written to describe how measurements should be taken. One author, a senior trainee in radiation oncology (observer 1), measured all available images. Another, a consultant neuro-radiologist (observer 2), measured distances for the first 5 patients on the database giving 30 data points for comparative analysis.
Results: Measurements of the HC were difficult and unreliable therefore only measurements of IAM and JF were used for comparison between 2 observers. The mean distances for observers 1 and 2 respectively were 12.4mm and 12.0mm (IAM) and 8.0mm and 7.8mm (JF). Differences between measurements were normally distributed; a Band-Altmann analysis was used to assess agreement. A bias of +0.3mm was found for observer 1 relative to observer 2. The 95% confidence interval for disagreement was -0.4mm to 1.05mm; this was felt to be clinically acceptable. The mean distances of CSF flow in the sample were 12.2mm (95% CI 8.8 – 15.6mm) for IAM and 7.3mm (95% CI 4.0 – 10.6mm) for JF. The distribution of data for the HC was bimodal with peaks around 2-4mm and 8-10mm, precluding useful analysis. This was because many scans stopped around or just beyond the HC's, resulting in poor image quality. We surmise that longer measurements come from scans where the HC was fully included.
Conclusions: FIESTA MRI gives excellent views of the posterior fossa CN foraminae and the CSF within. Measurement of these spaces is robust and reproducible. We intend to use these data to analyse previous treatment plans for both medulloblastoma and ependymoma and investigate whether specific voluming of these structures has any impact on target coverage and whether the CSF in these spaces may have been under-treated.

OC-0561

Hypothesis-generating prospective study for auto-delineation in lung tumors: READY LUNG-01

C. Valentini[1], L. Boldrini[1], G. Chiloiro[1], G.C. Mattiucci[1], G. Mantini[1], D. Pasini[1], N. Dinapoli[1], N. Caria[2], V. Valentini[1]
[1]*Catholic University of Sacred Heart, Radiation Oncology, Rome, Italy*
[2]*Varian Medical System, Medical Solution, Palo Alto (CA), USA*

Purpose/Objective: READY (REsearch program in Auto Delineation sYstem)-LUNG01 is an hypothesis-generating prospective study, which has the aim to validate in clinical